An Iterative Method for Solving the Inverse Problem in Electrocardiography Imaging : From Body Surface to Heart Potential

Nejib Zemzemi[1], Hamed Bourenane[2] , Hubert Cochet[3]

[1]INRIA Bordeaux Sud-Ouest, Talence, France
[2] Université de Bordeaux, Bordeaux, France
[3] CHU de Bordeaux, Pessac, France

Abstract

Solving the inverse problem in electrocardiography imaging (ECGI) is a challenging problem. In this work, we present an ECGI solver based on the iterative Kozlov-Maz'ya-Fomin (KMF) method. Because of the lack of gold standards data for this problem, we propose to test this method on synthetical data generated based on the bidomain state-of-the-art model. We segmented a real geometry of a 43 years old women and produced a computational geometry on which we run the forward problem body surface potentials BSPs. We analyse the reconstructed solution using the Relative error in time and space, the correlation coefficient and phase mapping procedure.

1. Introduction

One of the most recent heart imaging techniques introduced recently to the clinical industry is the electrocadiography imaging (ECGI). This technique allows a non-invasive reconstruction of the electrical potential on the heart surface based on electrical potential measurement on the body surface and anatomical data of the torso. It has been a research topic for decades and it is now under clinical assessment in different leading hospitals around the world. ECGI provides very precious informations about the heart condition since it is able to provide refined spatial description of the electrical wave pathway and magnitude on the heart surface. This helps a lot in different clinical interventions like radio-frequency ablation usually used to stop atrial and ventricular arrhythmias. An accurate ECGI tool allows a very good spacial targeting of cardiac arrhythmias and thus it helps to make more accurate clinical interventions. The scientific algorithms behind any ECGI tool are able to pre-process the anatomical data of the patient in order to provide a computational mesh, filter noisy measurements of the electrical potential but also solve an inverse problem.

However, the non-invasive reconstruction of the epicardial potential is not strait forward. The difficulty in the reconstruction of electrical potential on the heart surface is mainly due to the the ill poseddness of the mathematical problem behind the reconstruction. It has been known, since nine decades [1] mathematically ill posed in the sense that a small perturbation on the measured potential could generate a high perturbation on the reconstructed potential. Different works treated this problem [2–4] based on boundary element method for the discretization and Thikhonov regularization techniques to ensure the well posedness of the mathematical problem.

In this paper we propose an other approach of treating the inverse problem in electrocardiography based on the KMF method used to solve the Cauchy problem [5]. We make use numerical simulations in order to build a gold standard data that would be used to test the KMF algorithm. Our forward problem simulations are based on the state-of-the-art bidomain model which has been successfully used to generate body surface potentials in normal and pathological conditions [6] and for rem-entree simulations [7]. This allow as to generate electrical potentials in the heart and in the torso. We generated a normal heart beat and a reentry heart wave using the S1S2 protocol. We extract the heart surface elctrical potential and on the body surface potentials. We consider this data as our Gold standard. We then add different levels of noise to the BSPs and we solve the inverse problem using the KMF method. We compare the obtained solution to the gold standard electrograms.

2. Methods

The forward problem is solved based on the bidomain model in the cardiac tissue. In order to produce body surface potentials we solve the diffusion equation in the torso domain taking as a boundary condition the extracellular potential at the heart torso interface. On the external boundary of the torso we take a non flux boundary condition. Details about the models and numerical methods could be found in [6]). In this section we present at first the

anatomical model constructed from medical images, then we present the mathematical formulations and numerical methods that we will use to solve the inverse problem.

2.1. Anatomical model

We use a geometry that we have segmented from a CT scan of a 43 year old woman. The DICOM images were segmented using the medical imaging software Osirix. We identify three regions in the torso domain: lungs, bones, and the rest of the torso tissue. After segmentation, we use we use Tetgen and INRIA meshing Software MMG3D in order to get a good quality of athetrahedral mesh.

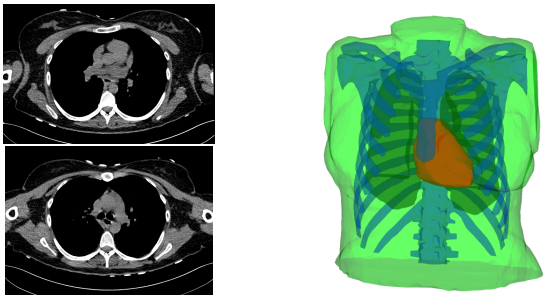

Figure 1. Two slices of the CT-scan images (left). Torso geometry showing the epicardium (heart-torso interface Σ) (red), lungs (yellow) bones (blue) and torso external boundary Γ_{ext} (green).

2.2. Inverse problem

ECGI allows to construct the electrical potential on the heart surface Σ from data measured on the body surface Γ_{ext}. We assume that the electrical potential is governed by the diffusion equation in the torso as shown in the previous paragraph. For a given potential data T measured on the body surface Γ_{ext}, the goal is to find u_{e} on Σ such that the potential data in the torso domain satisfies

$$\begin{cases} \operatorname{div}(\boldsymbol{\sigma}_{\text{T}} \boldsymbol{\nabla} u_{\text{T}}) = 0, \text{ in } \Omega_{\text{T}}, \\ \boldsymbol{\sigma}_{\text{T}} \boldsymbol{\nabla} u_{\text{T}}.\boldsymbol{n} = 0, \text{ and } u_{\text{T}} = T, \text{ on } \Gamma_{\text{ext}}, \\ u_{\text{T}} = u_{\text{e}}, \text{ on } \Sigma. \end{cases} \tag{1}$$

This problem is ill posed because the u_{T} is over determined on the boundary Γ_{ext}, where we have two boundary conditions to be satisfied. In order to find u_{e}, we use the KMF iterative method which works as a filter of the ill posedness [5, 8] . For a given electrical potential distribution on the body surface T and an initial guess about u^0, we can build tow sequences (v^n, u^n) as follows

$$\begin{cases} \operatorname{div}(\boldsymbol{\sigma}_{\text{T}} \boldsymbol{\nabla} v^{n+1}) = 0, \text{ in } \Omega_{\text{T}}, \\ \boldsymbol{\sigma}_{\text{T}} \boldsymbol{\nabla} v^{n+1}.\boldsymbol{n} = 0, \text{ on } \Gamma_{\text{ext}}, \\ v^{n+1} = u^n, \text{ on } \Sigma. \end{cases} \tag{2}$$

$$\begin{cases} \operatorname{div}(\boldsymbol{\sigma}_{\text{T}} \boldsymbol{\nabla} u^{n+1}) = 0, \text{ in } \Omega_{\text{T}}, \\ u^{n+1} = T, \text{ on } \Gamma_{\text{ext}}, \\ \boldsymbol{\sigma}_{\text{T}} \boldsymbol{\nabla} u^{n+1}.\boldsymbol{n} = \boldsymbol{\sigma}_{\text{T}} \boldsymbol{\nabla} v^{n+1}.\boldsymbol{n}, \text{ on } \Sigma. \end{cases} \tag{3}$$

The flux of v^{n+1}, solution of equation (2), depends linearly on u^n. We denote by S_N the Dirichlet to Neumann application that maps ${u^n}_{/\Sigma}$ to $(\boldsymbol{\sigma}_{\text{T}} \boldsymbol{\nabla} v^{n+1}.\boldsymbol{n})_{/\Sigma}$,

$$(\boldsymbol{\sigma}_{\text{T}} \boldsymbol{\nabla} v^{n+1}.\boldsymbol{n})_{/\Sigma} = S_N * {u^n}_{/\Sigma}.$$

On the other hand the application that maps v^{n+1} to u^{n+1} solution of equation (3) is affine and could be written as follows,

$$u^{n+1}_{/\Sigma} = S_D(\boldsymbol{\sigma}_{\text{T}} \boldsymbol{\nabla} v^{n+1}.\boldsymbol{n})_{/\Sigma} + S_{rhs} T,$$

where S_D is the Neumann to Dirichlet operator and $S_D(\boldsymbol{\sigma}_{\text{T}} \boldsymbol{\nabla} v^{n+1}.\boldsymbol{n})_{/\Sigma}$ is solution of the following problem

$$\begin{cases} \operatorname{div}(\boldsymbol{\sigma}_{\text{T}} \boldsymbol{\nabla} u) = 0, \text{ in } \Omega_{\text{T}}, \\ u = 0, \text{ on } \Gamma_{\text{ext}}, \\ \boldsymbol{\sigma}_{\text{T}} \boldsymbol{\nabla} u.\boldsymbol{n} = \boldsymbol{\sigma}_{\text{T}} \boldsymbol{\nabla} v^{n+1}.\boldsymbol{n}, \text{ on } \Sigma. \end{cases} \tag{4}$$

The operator S_{rhs} maps the BSP T to the residual part $S_{rhs}T$, the solution of the following problem on Σ

$$\begin{cases} \operatorname{div}(\boldsymbol{\sigma}_{\text{T}} \boldsymbol{\nabla} u) = 0, \text{ in } \Omega_{\text{T}}, \\ u = T, \text{ on } \Gamma_{\text{ext}}, \\ \boldsymbol{\sigma}_{\text{T}} \boldsymbol{\nabla} u.\boldsymbol{n} = 0, \text{ on } \Sigma. \end{cases} \tag{5}$$

Note that if we consider a static geometry, operators S_N, S_D and S_{rhs} are computed once for all, since they depend only on the mesh and the conductivities in the torso represented by $\boldsymbol{\sigma}_{\text{T}}$. Computing S_N, S_D and S_{rhs} avoids solving a 3D finite element problem at each iteration and allows a real time solving of the inverse problem.

3. Numerical results

We start by generating synthetic data using an ECG simulator based on the bidomain model. We generate BSPs for two heart cases, a healthy and a fibrillation conditions. The model parameters are the same in both cases they only differ by the stimulation protocols: In the first case, the heart is stimulated in the apex and the electrical wave propagates from apex to base. We refer to this simulation as a normal or healthy case. In the second case we apply a S1-S2 protocol, in order to produce a re-entry wave, we refer to this

case as a fibrillation or re-entree case. These two cases will be considered as our gold standard data. Further informations about the forward problem modelling could be found in [6]. For each time step, we extract BSPs, we add 5% of noise and we use it as the given data T. we then solve the inverse problem following the KMF method explained in the previous paragraph. In Fig.2 (respectively, Fig.3), we show snapshots of the electrical potential distribution in the body (including heart surface and torso volume), in these snapshots we compare the inverse solution to the gold standard normal (respectively, re-entree) case.

The distribution of the reconstructed electrical potential

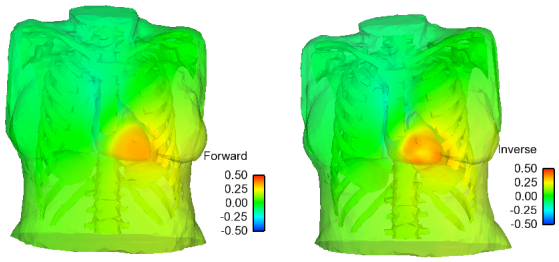

Figure 2. Snapshots of the potential distribution in the normal case. Forward solution (left) and Inverse solution (right). The color bar scale is in mV.

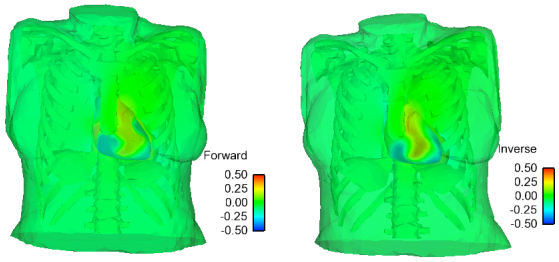

Figure 3. Snapshots of potential distribution for re-entry case. Forward solution (left) and Inverse solution (right). The color bar scale is in mV.

is synchronized with the gold standard electrical potential distribution in both normal and re-entree cases. We remark that the wave front is well captured but in the inverse solution it is much more smoother than in the exact solution. As shown in previous study [7], the wave front in the normal case is much accurate than in the re-entree case. Hence we will focus our study on the re-entree case. In Fig.4 (left) (respectively right), we show a comparison between the inverse and the exact solutions of the heart potential time course at a point located in the left (respectively right) epicardium. Although signals are synchronized in both location, the magnitude of the electrical potential is clearly more accurate in the right ventricle than it is in the left one. In Fig.5 (left) (respectively, right), we show the spa-

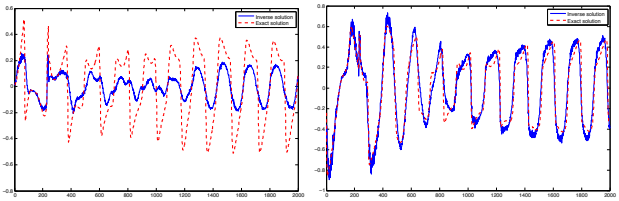

Figure 4. Left (respectively, right): Comparison of exact (red) and inverse (blue) solutions at a given point located in the surface the left (respectively right) ventricle in the re-entree case. X-axis: time (ms) and Y-axis: potential (mV)

tial distribution of the relative error in time by computing the l^2 relative error in time at each point of the heart surface geometry. We see that the error is much higher in the left ventricle where its maximum reaches 75% while in the right ventricle surface it doesn't exceed 35%. In Fig

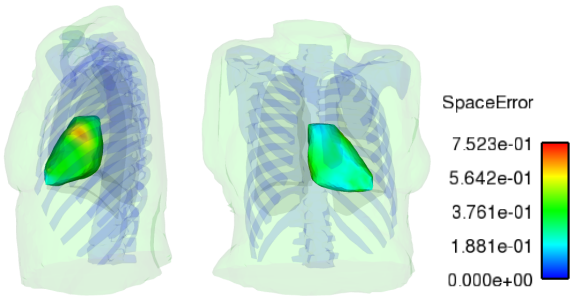

Figure 5. Left (respectively, right): left (respectively, right) ventricle view of the heart showing the l^2 relative error in time at each point of the geometry. The color bar is dimensionless.

6 (left), we show the time evolution of the space relative error by computing at each time step the spatial l^2 relative error. The mean of the relative error both in space and time is 0.45. In In Fig 6 (right), we show the time evolution of the correlation coeficient (CC) which gives an idea about the spatial correlation of the inverse solution to the gold standard data. The mean of the CC in time is 0.92. The inverse solution is 92% accurate in terms of the pattern of activation. At each point of the geometry we also compute the phase mapping of the inverse solution based on the Hilbert transform. In Fig. 7 (left) (respectively, right), we show a right ventricle view of the spatial distribution of the phase map of the gold standard solution (respectively, inverse problem solution) at time 1000 ms. We remark that the phase is correctly reconstructed which is in agreement with the results of the CC shown in Fig. 6. In Fig. 8 (left) (respectively, right), we compare the exact and the inverse solutions phases at a location on the left (respectively right) ventricle. These phases correspond to the electrical poten-

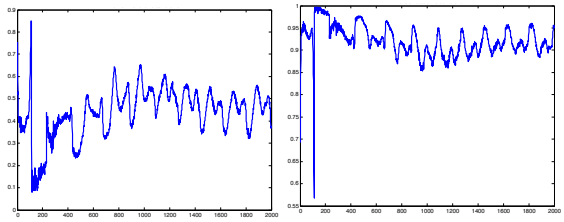

Figure 6. Time course of the relative error (left) and correlation coefficient (right) computed using the exact and inverse solutions in case of fibrillating heart conditions. X-axis: time (ms) and Y-axis: (dimensionless).

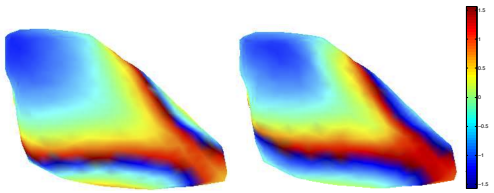

Figure 7. Right ventricle view: Snapshots of the phase map distribution in the re-entry case at time 1000 ms. Forward solution (left) and Inverse solution (right). The color bar scale is in Rad.

tials shown in Fig.4.

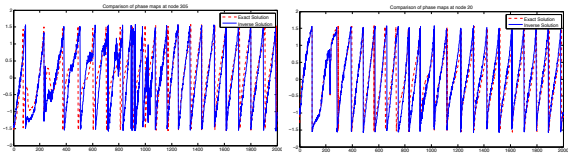

Figure 8. Left (respectively, right): Comparison of the signal phase for exact (red) and inverse (blue) solutions at a given point located in the surface the left (respectively right) ventricle in the re-entree case. X-axis: time (ms) and Y-axis: phase (Rad).

4. Discussion

In the present work we showed an alternative to the least square approach which has been intensively used in the electorocardiography imaging community. This is the first time that the KMF algorithm is used for solving the ECGI inverse problem. We have shown that in some regions the electrical potential is accurately computed in terms of magnitude whereas in other regions there is a hight loss in the magnitude of the constructed potential mainly in the right ventricle. When the magnitude of the potential is too low the effect of noise is clearly seen on the phase map as seen in Figures 4 (left) and 8 (left) in the time window between 750 ms and 1200 ms. Even though the pattern of activation is still accurate since the mean of the CC is 0.92.

5. Conclusion

In this paper, we presented a new approach for solving the inverse problem in electrocardiography. The method is based on the Kozlov-Maz'ya-Fomin algorithm. We segmented a 3D-anatomical model of a 43 years old women torso and use it for computation. We generated synthetic gold standard data using the bidomain model for sinus rhythm and re-entree. We focused our study on the re-entree case by post processing the inverse solutions: We have compared the relative error in time and in space. We have shown the locations where the potential is not accurately reconstructed. We plotted the correlation coeficient at each time step and compared the phase maps. The assessment of the KMF method on synthetical data is a first step and regarding the results obtained in this work, we think that this method is that there is an important potential for this method to be tested in clinical applications.

References

[1] Hadamard J. Lectures on Cauchy's problem in linear partial differential equations. Yale University Press, 1923.

[2] Zakharov E, Kalinin A. Algorithms and numerical analysis of dc fields in a piecewise-homogeneous medium by the boundary integral equation method. Computational Mathematics and Modeling 2009;20(3):247–257.

[3] Ghosh S, Rudy Y. Application of l1-norm regularization to epicardial potential solution of the inverse electrocardiography problem. Annals of Biomedical Engineering 2009; 37(5):902912.

[4] Denisov A, Zakharov E, Kalinin A, Kalinin V. Numerical methods for some inverse problems of heart electrophysiology. Differential Equations 2009;45(7):1034–1043.

[5] Kozlov VA, Maz'ya VG, Fomin A. An iterative method for solving the cauchy problem for elliptic equations. Zhurnal Vychislitelnoi Matematiki i Matematicheskoi Fiziki 1991; 31(1):64–74.

[6] Zemzemi N. Étude théorique et numérique de l'activité électrique du cœur: Applications aux électrocardiogrammes. Ph.D. thesis, Université Paris XI, 2009.

[7] Zemzemi N. An iterative method for solving the inverse problem in electrocardiography in normal and fibrillation conditions: A simulation study. In International Conference of Electrocardiology (ICE), 2014. International Society of Electrocardiology, 2014; 53–56.

[8] Lesnic D, Elliott L, Ingham D. An iterative boundary element method for solving numerically the cauchy problem for the laplace equation. Engineering analysis with boundary elements 1997;20(2):123–133.

Address for correspondence:

Nejib Zemzemi, INRIA Bordeaux Sud-Ouest
200 rue de la vieille tour 33405 Talence. France
nejib.zemzemi@inria.fr